LUND UNIVERSITY

Analysis of large finite periodic structures using infinite periodicity methods

Sjöberg, Daniel

2006

Link to publication

Citation for published version (APA):
Sjöberg, D. (2006). *Analysis of large finite periodic structures using infinite periodicity methods*. (Technical Report LUTEDX/(TEAT-7143)/1-22/(2006); Vol. TEAT-7143). [Publisher information missing].

Total number of authors:
1

General rights
Unless other specific re-use rights are stated the following general rights apply:
Copyright and moral rights for the publications made accessible in the public portal are retained by the authors and/or other copyright owners and it is a condition of accessing publications that users recognise and abide by the legal requirements associated with these rights.
• Users may download and print one copy of any publication from the public portal for the purpose of private study or research.
• You may not further distribute the material or use it for any profit-making activity or commercial gain
• You may freely distribute the URL identifying the publication in the public portal

Read more about Creative commons licenses: https://creativecommons.org/licenses/

Take down policy
If you believe that this document breaches copyright please contact us providing details, and we will remove access to the work immediately and investigate your claim.

LUND UNIVERSITY

PO Box 117
221 00 Lund
+46 46-222 00 00

CODEN:LUTEDX/(TEAT-7143)/1-22/(2006)

Analysis of large finite periodic structures using infinite periodicity methods

Daniel Sjöberg

Department of Electroscience
Electromagnetic Theory
Lund Institute of Technology
Sweden

Daniel Sjöberg
daniel.sjoberg@es.lth.se

Department of Electroscience
Electromagnetic Theory
Lund Institute of Technology
P.O. Box 118
SE-221 00 Lund
Sweden

Editor: Gerhard Kristensson
© Daniel Sjöberg, Lund, February 17, 2006

Abstract

We present a method for studying large finite periodic structures using software developed for infinite periodic structures. The method is based on the Floquet-Bloch transformation, which splits the spatial description into one microscopic spatial variable inside the unit cell, and one macroscopic wave vector describing the variations on a scale encompassing many unit cells. The resulting algorithm is iterative, and solves an infinite periodic problem in each step, where the sources have been filtered through a windowing function. The computational cost for the iterations is negligible compared to computing the impedance matrices for the infinite periodic problems, and it is shown that the algorithm converges if the periodic structure is large enough.

1 Introduction

Computations involving large finite arrays present a formidable problem, and have indeed inspired much computational research during the years, ever pressing the limits of modern computers. In this paper we present a systematic formalism for treating this case based on the assumption that we have a reasonably fast method for treating the infinite periodic case, which permits us to reduce the calculations to a single unit cell.

Through the years, various attempts have been made at solving such problems, and the recent thesis by Bekers [2, Ch. 1] provides a thorough review. Essentially, the problem resides in the fact that since the structure is large, it has many degrees of freedom that must be modeled. Even if we could accurately describe the interaction between each degree of freedom, they may be so many that it is impossible to even fit the problem in the memory of a computer.

One way of approaching the problem is to solve the full problem, but taking special care to identify known redundancies in coupling between the elements. This is the great benefit of methods like the Fast Multipole Method (FMM) [7], Adaptive Integral Method (AIM) [3], or the Array Decomposition Method (ADM) [14, 15]. Since these methods describe the full problem, their memory requirements increase with the size of the periodic structure.

It is common to take edges of the array into account by introducing diffraction fields originating from discontinuities in the array [5, 6, 18, 19]. In this approach, the fields are obtained from asymptotic evalutation of integral representations, much in the same way as in the geometrical theory of diffraction (GTD). Since it is assumed that the edge behavior does not depend on the size of the structure, the computational requirements do not grow with the structure.

Another family of approaches is to make use of the infinite array analysis, and apply the finiteness of the array as various corrections to this. The easiest to understand is probably the windowing technique originating in [13, 22–24], which essentially takes the result from the infinite array case and convolves it in the spectral domain with the Fourier transform of the characteristic function of the array domain. Whereas this provides some useful information on the finiteness of the periodic

structure, there is one fundamental flaw due to the fact that each unit cell effectively experiences a surrounding corresponding to the center of the structure. This can also be seen as the consequence of assuming the currents in an entire unit cell to be proportional to the current in a fundamental unit cell.

Bekers [2] in his turn, proposes a hierarchical way of thinking of the array. Eigencurrents are first determined for the elements, and are then used as basis functions for finding eigencurrents on subarrays, which are in turn used as basis functions in higher subarrays and so on. The modularity of this method shows great potential, but since the eigencurrents are calculated from the single, isolated elements, it is not clear to this author if the method can treat cases where current may flow between the elements.

When discussing finite periodic structures, it would be a shame not to mention Munk's book [17]. Although he mainly discusses simple wire dipoles, he proposes a very useful and intuitive physical interpretation of the characteristics of a finite periodic structure. He identifies three currents on a finite structure: 1) the Floquet currents that would be present on an infinite structure, 2) surface waves propagating on the structure, possibly interfering constructively to form standing waves, and 3) end currents, located near the edges of the structure, identified as reflections of the surface waves. The main thing is that the surface waves may not appear on the infinite structure, but they *do* in general appear on the finite one. Although the surface waves can be characterized by methods based on infinite periodicity, there is in general no way of computing the strength of the surface waves unless we can solve the entire problem for the finite periodic structure, or approximate it with a finite-by-infinite structure [17, 25].

In this paper, we propose yet another method to study finite periodic structures, which does take surface waves into account. It is based on converting Maxwell's equations describing the full problem, to a problem defined in a unit cell, using the Floquet-Bloch transformation [4, 9, 20, 21]. This transformation provides a systematic way of simultaneously describing a microscopic scale and a macroscopic scale, where the microscopic scale is described by a spatial variable inside the unit cell, and the macroscopic scale is described in the Fourier domain, *i.e.*, by wave numbers corresponding to wave lengths larger than the unit cell. It is noteworthy that Bloch actually developped his version of Floquet's theory in order to be able to treat *finite* crystals.

There is no loss of information in the Floquet-Bloch transformation, and hence we still have to solve a large number of problems and store lots of data. However, the nice thing is that we are now able to separate the computations regarding the unit cell, containing the generic antenna element, and the large scale computations, which are concerned with the interaction with the finiteness of the structure. This not only provides a possibility to parallelize the problem to a high degree, but since the large scale is essentially described in the Fourier domain, the memory requirements of the algorithm do not necessarily increase with the size of the structure.

The method is rather similar to the windowing technique described above, but does not assume the current in each unit cell to be proportional to the current in a fundamental unit cell. Instead, the finiteness of the structure is taken into account

through an iterative solution, where a problem with infinite periodicity should be solved in each step, and the current sources at each step are essentially filtered with the window function in the spectral domain concerned with the large scale variations.

We have made an effort to keep the presentation as general as possible, in order not to get involved in distressing sidetracks. Hence, we discuss periodicity with an arbitrary lattice in one, two, and three dimensions simultaneously, and the shape of the periodic structure is arbitrary. The algorithm is largely independent of the particular numerical method used to solve the infinite periodic problem, although we primarily think of the moment method when discussing the computational complexity. We have also chosen not to include the possible sidetrack of including a taper on the periodic structure. In line with this aspiration for general results, we emphasize that the possible applications of this paper are not restricted to array antennas. Any finite periodic structure can be analyzed by this method, for instance a finite frequency selective surface (FSS), finite photonic bandgap crystals (PBG), or indeed nonresonant periodic structures representing the microscopic structure in materials, which is a common model in homogenization theory [20, 21].

This paper is organized as follows. In Section 2 we introduce a six-vector notation which significantly shortens the space necessary to discuss the electromagnetic field, as well as the pertinent notation for describing periodic media with an arbitrary lattice. The Floquet-Bloch transformation is presented in Section 3, and the unit cell problem is derived. The solution of the unit cell equation is discussed in Section 4, where we also discuss how to take eigenwaves into account through an integral equation. These eigenwaves are interpreted as the surface waves in Munk's phenomenology described above. In Section 5 we present the iterative scheme which is used to take the finite structure into account, and sections 6 and 7 are spent discussing the convergence of this scheme. Finally, we make some notes on the possible implementation of the algorithm in Section 8, and give our conclusions in Section 9. In the Appendix, we have gathered some results which are used throughout the paper and some lengthy derivations.

2 Notation

For notational convenience, we use scaled fields in this paper, *i.e.*, the SI-unit fields $\boldsymbol{E}_{\mathrm{SI}}$, $\boldsymbol{H}_{\mathrm{SI}}$, $\boldsymbol{D}_{\mathrm{SI}}$, and $\boldsymbol{B}_{\mathrm{SI}}$ are related to the fields $\boldsymbol{E}$, $\boldsymbol{H}$, $\boldsymbol{D}$, and $\boldsymbol{B}$ used in this paper by

$$\boldsymbol{E}_{\mathrm{SI}}(\boldsymbol{x}, t_{\mathrm{SI}}) = \epsilon_0^{-1/2}\boldsymbol{E}(\boldsymbol{x}, t) \qquad \boldsymbol{H}_{\mathrm{SI}}(\boldsymbol{x}, t_{\mathrm{SI}}) = \mu_0^{-1/2}\boldsymbol{H}(\boldsymbol{x}, t) \tag{2.1}$$

$$\boldsymbol{D}_{\mathrm{SI}}(\boldsymbol{x}, t_{\mathrm{SI}}) = \epsilon_0^{1/2}\boldsymbol{D}(\boldsymbol{x}, t) \qquad \boldsymbol{B}_{\mathrm{SI}}(\boldsymbol{x}, t_{\mathrm{SI}}) = \mu_0^{1/2}\boldsymbol{B}(\boldsymbol{x}, t) \tag{2.2}$$

where the permittivity and permeability of vacuum are denoted by ϵ_0 and μ_0, respectively. The time is scaled according to $t = c_0 t_{\mathrm{SI}}$, where $c_0 = 1/\sqrt{\epsilon_0\mu_0}$ is the speed of light in vacuum. With this scaling, all the electromagnetic fields have the same physical dimension $\sqrt{\text{power/volume}}$, *i.e.*, $(\,\mathrm{J\,s^{-1}\,m^{-3}})^{1/2}$, and the space and time

variables $\boldsymbol{x}$ and t both have the physical dimension length (m). The corresponding relations for the current density $\boldsymbol{J}_{\mathrm{SI}}$ and the charge density ρ_{SI} are

$$\boldsymbol{J}_{\mathrm{SI}}(\boldsymbol{x}, t_{\mathrm{SI}}) = \mu_0^{-1/2} \boldsymbol{J}(\boldsymbol{x}, t), \quad \rho_{\mathrm{SI}}(\boldsymbol{x}, t_{\mathrm{SI}}) = \epsilon_0^{1/2} \rho(\boldsymbol{x}, t) \tag{2.3}$$

In these units, Maxwell's equations are

$$\begin{cases} \nabla \times \boldsymbol{E} + \partial_t \boldsymbol{B} = \boldsymbol{0} \\ \nabla \times \boldsymbol{H} - \partial_t \boldsymbol{D} = \boldsymbol{J} \end{cases} \tag{2.4}$$

which are supplemented by the continuity equation

$$\nabla \cdot \boldsymbol{J} + \partial_t \rho = 0 \tag{2.5}$$

2.1 Six-vector notation

We now introduce a six-vector notation, which considerably shortens the notation. We group the fields according to

$$\mathsf{e} = \begin{pmatrix} \boldsymbol{E} \\ \boldsymbol{H} \end{pmatrix}, \quad \mathsf{d} = \begin{pmatrix} \boldsymbol{D} \\ \boldsymbol{B} \end{pmatrix}, \quad \mathsf{j} = \begin{pmatrix} \boldsymbol{J} \\ \boldsymbol{0} \end{pmatrix}, \quad \varrho = \begin{pmatrix} \rho \\ 0 \end{pmatrix} \tag{2.6}$$

Collections of vectors like e, d, and j are called six-vectors in the following, and collections of scalars like ϱ are called two-scalars. On occasions, we also make reference to different parts of these vectors and scalars if they are associated with the electric or magnetic fields. This is indicated by indices e or h. For instance, we may describe a two-scalar as $\varrho = [\varrho_{\mathrm{e}}, \varrho_{\mathrm{h}}]^{\mathrm{T}}$, where ϱ_{e} and ϱ_{h} are traditional scalars.

Note that even though there are physical reasons to say that there are no magnetic charges, it may still be advantageous to include the possibility in the model. Indeed, sometimes it is *necessary* since we might be solving not the full problem but only a subproblem. In this case, sources which may appear non-physical at first sight can be used to provide a coupling between different parts of the problem. Examples are for instance the Born approximation and various scattering problems, where we need to be able to treat arbitrary current densities j and charge densities ϱ.

Define differential operators according to

$$\nabla \times \mathsf{J} \cdot \mathsf{e} = \begin{pmatrix} \boldsymbol{0} & -\nabla \times \mathbf{I} \\ \nabla \times \mathbf{I} & \boldsymbol{0} \end{pmatrix} \cdot \begin{pmatrix} \boldsymbol{E} \\ \boldsymbol{H} \end{pmatrix} = \begin{pmatrix} -\nabla \times \boldsymbol{H} \\ \nabla \times \boldsymbol{E} \end{pmatrix}, \quad \nabla \cdot \mathsf{d} = \begin{pmatrix} \nabla \cdot \boldsymbol{D} \\ \nabla \cdot \boldsymbol{B} \end{pmatrix} \tag{2.7}$$

where $\mathbf{I}$ is the identity matrix in three dimensions. The large finite structure is modeled by material parameters $\mathsf{M}(\boldsymbol{x})$ varying in space, where the material is described by the constitutive relations

$$\mathsf{d}(\boldsymbol{x}, t) = \mathsf{M}(\boldsymbol{x}) \cdot \mathsf{e}(\boldsymbol{x}, t) + \int_{-\infty}^{t} (\boldsymbol{\sigma}(\boldsymbol{x}) + \boldsymbol{\chi}(\boldsymbol{x}, t - t')) \cdot \mathsf{e}(\boldsymbol{x}, t') \, \mathrm{d}t' \tag{2.8}$$

The optical response of the medium is then modeled by the real, symmetric, positive definite matrix $\mathsf{M}(\boldsymbol{x})$, the conduction currents are modeled by the real, symmetric,

positive semi-definite conductivity matrix $\boldsymbol{\sigma}(\boldsymbol{x})$, and the remaining dispersive effects (such as resonances or relaxation processes) are modeled by the susceptibility kernel $\boldsymbol{\chi}(\boldsymbol{x}, t)$. The Laplace transform and its inverse are defined as [1, Ch. 15]

$$f(s) = \int_0^\infty \mathrm{e}^{-st} f(t)\,\mathrm{d}t, \quad f(t) = \frac{1}{2\pi\mathrm{i}} \int_{s\in\gamma} \mathrm{e}^{st} f(s)\,\mathrm{d}s \tag{2.9}$$

where $\gamma = (\eta - \mathrm{i}\infty, \eta + \mathrm{i}\infty)$ is an integration path chosen so that the singularities of $f(s)$ are for $\operatorname{Re} s < \eta$. With the Laplace transform we have the usual relations $\partial_t \to s$, $\int_{-\infty}^t \to 1/s$, and convolutions become products, which is used to write

$$\mathsf{d}(\boldsymbol{x}, s) = (\mathsf{M}(\boldsymbol{x}) + \boldsymbol{\sigma}(\boldsymbol{x})/s + \boldsymbol{\chi}(\boldsymbol{x}, s)) \cdot \mathsf{e}(\boldsymbol{x}, s) = \mathsf{M}_\mathrm{c}(\boldsymbol{x}, s) \cdot \mathsf{e}(\boldsymbol{x}, s) \tag{2.10}$$

In order to guarantee a passive medium, *i.e.*, one that does not generate energy, we require [10, p. 15]

$$\operatorname{Re}(s\mathsf{M}_\mathrm{c}(\boldsymbol{x}, s)) \geq 0 \quad \forall \boldsymbol{x} \in \mathbb{R}^3,\ \operatorname{Re} s \geq 0 \tag{2.11}$$

In the following, we often write $\mathsf{M}_\mathrm{c}(\boldsymbol{x})$ or M_c with the s- and $\boldsymbol{x}$-dependence implicitly understood. Maxwell's equations and the continuity equation are then compactly written in the Laplace domain as

$$(\nabla \times \mathsf{J} + s\mathsf{M}_\mathrm{c}) \cdot \mathsf{e} + \mathsf{j} = \boldsymbol{0}, \quad \nabla \cdot \mathsf{j} + s\varrho = 0 \tag{2.12}$$

2.2 Infinite periodic structures

To lay down some notation, we temporarily assume the structure is infinite periodic, and denote the corresponding material matrix by $\mathsf{M}_\mathrm{c}^\#(\boldsymbol{x}, s)$. Although we start our formulation as if the structure is periodic in all three spatial dimensions, our applications are concerned with structures which may be periodic in one, two, or three dimensions. In most cases, this changes the notation only in an obvious manner.

The unit cell is denoted with U, and the periodic material satisfies $\mathsf{M}_\mathrm{c}^\#(\boldsymbol{x} + \boldsymbol{x}_{\boldsymbol{n}}, s) = \mathsf{M}_\mathrm{c}^\#(\boldsymbol{x}, s)$, $\boldsymbol{n} \in \mathbb{Z}^3$, where $\boldsymbol{x}_{\boldsymbol{n}} = n_1\boldsymbol{a}_1 + n_2\boldsymbol{a}_2 + n_3\boldsymbol{a}_3$ and $\boldsymbol{a}_i$, $i = 1, 2, 3$, are the basis vectors for the lattice. The reciprocal unit cell is denoted with U', and a vector in the reciprocal lattice is $\boldsymbol{k}_{\boldsymbol{n}} = n_1\boldsymbol{b}_1 + n_2\boldsymbol{b}_2 + n_3\boldsymbol{b}_3$, where $\boldsymbol{b}_1 = \frac{2\pi}{|U|}\boldsymbol{a}_2 \times \boldsymbol{a}_3$, $\boldsymbol{b}_2 = \frac{2\pi}{|U|}\boldsymbol{a}_3 \times \boldsymbol{a}_1$, $\boldsymbol{b}_3 = \frac{2\pi}{|U|}\boldsymbol{a}_1 \times \boldsymbol{a}_2$, and $|U| = \boldsymbol{a}_1 \cdot (\boldsymbol{a}_2 \times \boldsymbol{a}_3)$. This implies $\boldsymbol{a}_i \cdot \boldsymbol{b}_j = 2\pi\delta_{ij}$, where δ_{ij} is the Kronecker delta. For more on the description of periodic media, see the introductory chapters in most books on solid state physics, for instance [16]. We denote the typical length of the unit cell by a, *i.e.*, the physical vectors $\boldsymbol{a}_{1,2,3}$ and $\boldsymbol{b}_{1,2,3}$ can be expressed in dimensionless vectors $\hat{\boldsymbol{a}}_{1,2,3}$ and $\hat{\boldsymbol{b}}_{1,2,3}$ through the scaling $\boldsymbol{a}_{1,2,3} = a\hat{\boldsymbol{a}}_{1,2,3}$ and $\boldsymbol{b}_{1,2,3} = a^{-1}\hat{\boldsymbol{b}}_{1,2,3}$, where the dimensionless vectors $\hat{\boldsymbol{a}}_{1,2,3}$ have a typical length of 1.

For the definition of suitable function spaces for Maxwell's equations in infinite periodic media, we refer to [20].

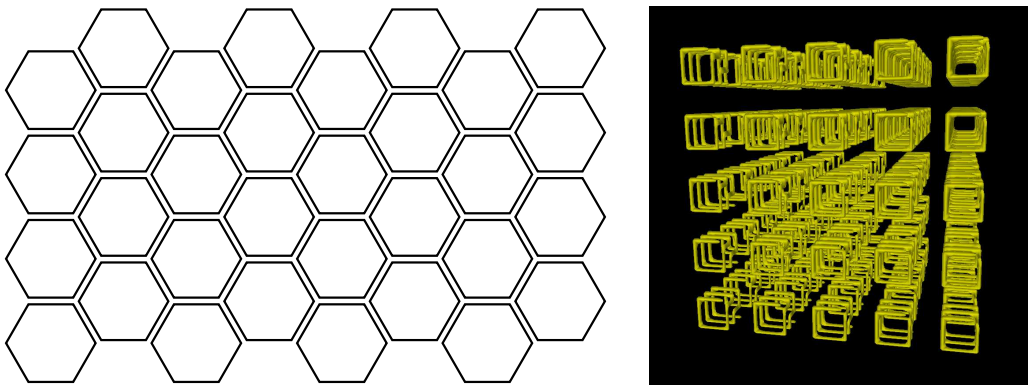

Figure 1: Example of two finite periodic structures. On the left, we have a frequency selective surface consisting of hexagonal metallic rings in a two-dimensional triangular lattice. On the right, we have a finite crystal with spiral inclusions in a simple cubic lattice.

2.3 Finite periodic structures

We will now assume that the structure can be considered as a finite segment of an infinite periodic structure as in Figure 1, *i.e.*, the lattice vectors $\boldsymbol{x_n}$ only make sense for the finite set of indices $\boldsymbol{n}$ which satisfy $\boldsymbol{x_n} \in \Omega$, where Ω denotes the volume containing the structure. We model this by a window function $\zeta(\boldsymbol{x})$, satisfying

$$\zeta(\boldsymbol{x}) = \begin{cases} 0 & \boldsymbol{x} \in \Omega \\ 1 & \boldsymbol{x} \notin \Omega \end{cases} \tag{2.13}$$

The material parameters are then described by

$$\mathsf{M}_{\mathrm{c}}(\boldsymbol{x}, s) = \mathsf{M}_{\mathrm{c}}^{\#}(\boldsymbol{x}, s) + \zeta(\boldsymbol{x})(\mathsf{M}_0 - \mathsf{M}_{\mathrm{c}}^{\#}(\boldsymbol{x}, s)) \tag{2.14}$$

where we assumed that the surrounding medium is constant and can be modeled by the constant matrix M_0. For the common case where the surrounding medium is air or vacuum, we have $\mathsf{M}_0 = \mathsf{I}$, the identity matrix. Observe that this approach cannot account for tapering of the elements. To include a tapering at the boundary of the structure, we may further adjust (2.14) to include a layer which is nonzero only at the corresponding points. Note however, that it is perfectly feasible to include a tapering in the currents using the present form of (2.14).

3 Floquet-Bloch representation

In Appendix A some computational rules for the Floquet-Bloch representation of fields is given. Using this representation, the electromagnetic field can be written

$$\mathsf{e}(\boldsymbol{x}, s) = \frac{1}{|U'|} \int_{U'} \mathrm{e}^{\mathrm{i}\boldsymbol{k}\cdot\boldsymbol{x}} \tilde{\mathsf{e}}(\boldsymbol{x}, \boldsymbol{k}, s) \, \mathrm{d}v_{\boldsymbol{k}} \tag{3.1}$$

The Bloch amplitude $\tilde{\mathsf{e}}(\boldsymbol{x},\boldsymbol{k})$ is a U-periodic function of $\boldsymbol{x}$, and $\mathrm{e}^{\mathrm{i}\boldsymbol{k}\cdot\boldsymbol{x}}\tilde{\mathsf{e}}(\boldsymbol{x},\boldsymbol{k})$ is a U'-periodic function of $\boldsymbol{k}$. For an infinite periodic structure, Maxwell's equations for the Bloch amplitude are then

$$((\nabla+\mathrm{i}\boldsymbol{k})\times\mathsf{J}+s\mathsf{M}_{\mathrm{c}}^{\#})\cdot\tilde{\mathsf{e}}+\tilde{\mathsf{j}}=\mathbf{0},\quad \boldsymbol{x}\in U,\ \boldsymbol{k}\in U' \tag{3.2}$$

and the continuity equation is $(\nabla+\mathrm{i}\boldsymbol{k})\cdot\tilde{\mathsf{j}}+s\tilde{\varrho}=0$. The advantage with this formulation is that the differential equations only have to be solved in a unit cell U, although the price is paid through the fact that we must solve it for every $\boldsymbol{k}$ in the reciprocal unit cell U'. This is the kind of equation which programs developed for the infinite periodic case can solve.

We now assume that the structure is finite, *i.e.*, we use the representation (2.14) for the material matrix. According to Appendix A, the Floquet-Bloch transformation of a product between two non-periodic functions becomes a convolution over the reciprocal unit cell U'. This means the transform of $\mathsf{M}_{\mathrm{c}}\cdot\mathsf{e}$ is

$$\widetilde{[\mathsf{M}_{\mathrm{c}}\cdot\mathsf{e}]}(\boldsymbol{x},\boldsymbol{k},s)=\mathsf{M}_{\mathrm{c}}^{\#}(\boldsymbol{x},s)\cdot\tilde{\mathsf{e}}(\boldsymbol{x},\boldsymbol{k},s)+(\mathsf{M}_0-\mathsf{M}_{\mathrm{c}}^{\#}(\boldsymbol{x},s))\cdot\left[\frac{1}{|U'|}\tilde{\zeta}\overset{U'}{*}\tilde{\mathsf{e}}\right](\boldsymbol{x},\boldsymbol{k},s) \tag{3.3}$$

and we can write Maxwell's equations as

$$\boxed{((\nabla+\mathrm{i}\boldsymbol{k})\times\mathsf{J}+s\mathsf{M}_{\mathrm{c}}^{\#})\cdot\tilde{\mathsf{e}}=-\tilde{\mathsf{j}}+s(\mathsf{M}_{\mathrm{c}}^{\#}-\mathsf{M}_0)\frac{1}{|U'|}\tilde{\zeta}\overset{U'}{*}\tilde{\mathsf{e}}} \tag{3.4}$$

where the last term in the right hand side can be considered as a measure of the finiteness of the structure. The Bloch amplitude of the window function is

$$\tilde{\zeta}(\boldsymbol{x},\boldsymbol{k})=\sum_{\boldsymbol{n}\in\mathbb{Z}^3}\mathrm{e}^{-\mathrm{i}\boldsymbol{k}\cdot(\boldsymbol{x}+\boldsymbol{x}_{\boldsymbol{n}})}\zeta(\boldsymbol{x}+\boldsymbol{x}_{\boldsymbol{n}})=\sum_{\boldsymbol{n}\notin I}\mathrm{e}^{-\mathrm{i}\boldsymbol{k}\cdot(\boldsymbol{x}+\boldsymbol{x}_{\boldsymbol{n}})} \tag{3.5}$$

where I corresponds to the finite set of indices $\boldsymbol{n}$ describing the finite structure. For convenience, we will sometimes write this as

$$\tilde{\zeta}(\boldsymbol{x},\boldsymbol{k})=\mathrm{e}^{-\mathrm{i}\boldsymbol{k}\cdot\boldsymbol{x}}\left(\sum_{\boldsymbol{n}\in\mathbb{Z}^3}\mathrm{e}^{-\mathrm{i}\boldsymbol{k}\cdot\boldsymbol{x}_{\boldsymbol{n}}}-\sum_{\boldsymbol{n}\in I}\mathrm{e}^{-\mathrm{i}\boldsymbol{k}\cdot\boldsymbol{x}_{\boldsymbol{n}}}\right)=\mathrm{e}^{-\mathrm{i}\boldsymbol{k}\cdot\boldsymbol{x}}\Big(|U'|\delta(\boldsymbol{k})-\tilde{\zeta}_0(\boldsymbol{k})\Big) \tag{3.6}$$

where $\tilde{\zeta}_0(\boldsymbol{k})$ is a continuous function. As the window corresponding to the function ζ extends to all $\mathbb{R}^3$, the Bloch amplitude $\tilde{\zeta}$ approaches zero in the distribution sense, or $\tilde{\zeta}_0\to|U'|\delta(\boldsymbol{k})$, as we will see further on. A typical case is for a one-dimensional array of N elements with period a centered around the origin, where $\boldsymbol{x}_{\boldsymbol{n}}=(na-(N+1)a/2)\hat{\boldsymbol{x}}_1$ and $\boldsymbol{k}=k\hat{\boldsymbol{x}}_1$ with $k\in(-\pi/a,\pi/a)$, that is

$$\begin{aligned}\tilde{\zeta}_0(\boldsymbol{k})&=\sum_{\boldsymbol{n}\in I}\mathrm{e}^{-\mathrm{i}\boldsymbol{k}\cdot\boldsymbol{x}_{\boldsymbol{n}}}=\sum_{n=1}^{N}\mathrm{e}^{-\mathrm{i}k(na-(N+1)a/2)}=\mathrm{e}^{\mathrm{i}k(N+1)a/2}\frac{\mathrm{e}^{-\mathrm{i}ka}-\mathrm{e}^{-\mathrm{i}k(N+1)a}}{1-\mathrm{e}^{-\mathrm{i}ka}}\\&=\mathrm{e}^{\mathrm{i}k(N+1)a/2}\frac{1-\mathrm{e}^{-\mathrm{i}kNa}}{\mathrm{e}^{\mathrm{i}ka}-1}=\frac{\mathrm{e}^{\mathrm{i}kaN/2}-\mathrm{e}^{-\mathrm{i}kaN/2}}{\mathrm{e}^{\mathrm{i}ka/2}-\mathrm{e}^{-\mathrm{i}ka/2}}=\frac{\sin(Nka/2)}{\sin(ka/2)}\end{aligned} \tag{3.7}$$

With periodicity in higher dimensions, $\tilde{\zeta}_0$ is typically a product of such functions, one for each component of $\boldsymbol{k}$. The typical appearance of this factor is shown in Figure 2.

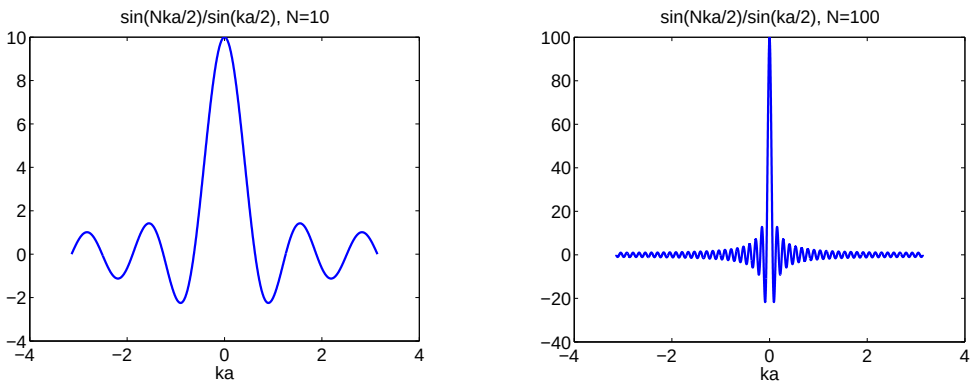

Figure 2: The function $\tilde{\zeta}_0(\boldsymbol{k}) = \frac{\sin(Nka/2)}{\sin(ka/2)}$ for $N = 10$ and $N = 100$.

4 Solving Maxwell's equations

We define the singular value decomposition of Maxwell's equations as [20]

$$((\nabla + \mathrm{i}\boldsymbol{k}) \times \mathsf{J} + s\mathsf{M}_{\mathrm{c}}^{\#}) \cdot \mathsf{u}_n = \sigma_n \mathsf{v}_n \tag{4.1}$$

$$(-(\nabla + \mathrm{i}\boldsymbol{k}) \times \mathsf{J} + (s\mathsf{M}_{\mathrm{c}}^{\#})^{\mathrm{H}}) \cdot \mathsf{v}_n = \sigma_n \mathsf{u}_n \tag{4.2}$$

with the singular values arranged in ascending order, *i.e.*,

$$0 \leq \sigma_1 \leq \sigma_2 \leq \cdots \tag{4.3}$$

The functions $\{\mathsf{v}_1\}_{n=1}^{\infty}$ and $\{\mathsf{u}_1\}_{n=1}^{\infty}$ are orthogonal sequences which constitute a basis for the range of the Maxwell operator and its adjoint, respectively. From the results for the vacuum operator, reported in the Appendix of [20], we assume that the null space of the operator is zero for all $\boldsymbol{k} \in U'$ except for some very special ones. These special $\boldsymbol{k}$ are contained in the set

$$\Gamma = \{\boldsymbol{k} \in U' : \ \sigma_1(\boldsymbol{k}) = 0\} \tag{4.4}$$

which corresponds to the occurrence of freely propagating waves in the infinite periodic structure, *i.e.*, the eigenwaves explored in [21]. In the case of array antennas, this corresponds to surface waves. Since different names can be attributed when considering different applications of periodic structures, we use the more neutral term eigenwaves in this paper. Once again inspired by the vacuum results, we note that for $s = \eta + \mathrm{i}\omega$, the smallest singular value is $\sigma_{1,\mathrm{vac}}(\boldsymbol{k}) = \sqrt{\eta^2 + (|\omega| - |\boldsymbol{k}|)^2}$, which means $\sigma_{1,\mathrm{vac}}(\boldsymbol{k}) = 0$ only for $\eta = 0$ and $|\boldsymbol{k}| = |\omega|$, *i.e.*, Γ_{vac} is always empty except for $s = \mathrm{i}\omega$, when it consists of the surface $|\boldsymbol{k}| = |\omega|$.

We now expand the electromagnetic field as

$$\tilde{\mathsf{e}}(\boldsymbol{x}, \boldsymbol{k}) = \sum_{n=1}^{\infty} e_n(\boldsymbol{k}) \mathsf{u}_n(\boldsymbol{x}, \boldsymbol{k}) \tag{4.5}$$

which implies $((\nabla + \mathrm{i}\boldsymbol{k}) \times \mathsf{J} + s\mathsf{M}_\mathrm{c}^\#) \cdot \tilde{\mathsf{e}} = \sum_{n=1}^\infty \sigma_n e_n \mathsf{v}_n$. In principle, the expansion coefficients can be determined from the equation

$$((\nabla + \mathrm{i}\boldsymbol{k}) \times \mathsf{J} + s\mathsf{M}_\mathrm{c}^\#) \cdot \tilde{\mathsf{e}} = -\tilde{\mathsf{j}} + s(\mathsf{M}_\mathrm{c}^\# - \mathsf{M}_0) \cdot \frac{1}{|U'|} \tilde{\zeta} \overset{U'}{*} \tilde{\mathsf{e}} \tag{4.6}$$

by taking the scalar product with v_n to find

$$e_n = \frac{1}{\sigma_n} \left(-\tilde{\mathsf{j}} + s(\mathsf{M}_\mathrm{c}^\# - \mathsf{M}_0) \cdot \frac{1}{|U'|} \tilde{\zeta} \overset{U'}{*} \sum_{n=1}^\infty e_n \mathsf{u}_n, \mathsf{v}_n \right) \tag{4.7}$$

which could be solved by iteration. However, since the smallest singular value σ_1 is zero when $\boldsymbol{k} \in \Gamma$, the factor $1/\sigma_1$ blows up for these $\boldsymbol{k}$, and this scheme cannot be immediately applied to the first expansion coefficient e_1.

We intend to find an integral equation for this expansion coefficient. Following the same procedure as before, we obtain the equation

$$\sigma_1 e_1 = \left(-\tilde{\mathsf{j}} + s(\mathsf{M}_\mathrm{c}^\# - \mathsf{M}_0) \cdot \frac{1}{|U'|} \tilde{\zeta} \overset{U'}{*} \sum_{n=1}^\infty e_n \mathsf{u}_n, \mathsf{v}_1 \right) \tag{4.8}$$

From (3.6) it is clear that there is a delta distribution in the Bloch amplitude of the window function,

$$\tilde{\zeta}(\boldsymbol{x}, \boldsymbol{k}) = \mathrm{e}^{-\mathrm{i}\boldsymbol{k}\cdot\boldsymbol{x}} \left(|U'| \delta(\boldsymbol{k}) - \tilde{\zeta}_0(\boldsymbol{k}) \right) \tag{4.9}$$

where $\tilde{\zeta}_0$ is a continuous function. Since the convolution with a delta distribution is the identity operation, we have

$$\left[\frac{1}{|U'|} \tilde{\zeta} \overset{U'}{*} \tilde{\mathsf{e}} \right] (\boldsymbol{x}, \boldsymbol{k}) = \tilde{\mathsf{e}}(\boldsymbol{x}, \boldsymbol{k}) - \frac{1}{|U'|} \int_{U'} \mathrm{e}^{-\mathrm{i}(\boldsymbol{k}-\boldsymbol{k}')\cdot\boldsymbol{x}} \tilde{\zeta}_0(\boldsymbol{k} - \boldsymbol{k}') \tilde{\mathsf{e}}(\boldsymbol{x}, \boldsymbol{k}') \, \mathrm{d}v_{\boldsymbol{k}'} \tag{4.10}$$

Using this in (4.8) and rearranging to get all terms involving e_1 in the left hand side, we get

$$\begin{aligned} &\underbrace{\left[\sigma_1(\boldsymbol{k}) - (s(\mathsf{M}_\mathrm{c}^\# - \mathsf{M}_0) \cdot \mathsf{u}_1, \mathsf{v}_1) \right]}_{=h(\boldsymbol{k})} e_1(\boldsymbol{k}) \\ &\qquad + \frac{1}{|U'|} \int_{U'} e_1(\boldsymbol{k}') \tilde{\zeta}_0(\boldsymbol{k} - \boldsymbol{k}') \underbrace{(s(\mathsf{M}_\mathrm{c}^\# - \mathsf{M}_0) \cdot \mathrm{e}^{\mathrm{i}\boldsymbol{k}'\cdot\boldsymbol{x}} \mathsf{u}_1, \mathrm{e}^{\mathrm{i}\boldsymbol{k}\cdot\boldsymbol{x}} \mathsf{v}_1)}_{=g(\boldsymbol{k},\boldsymbol{k}')} \, \mathrm{d}v_{\boldsymbol{k}'} \\ &\qquad = \underbrace{\left(-\tilde{\mathsf{j}} + s(\mathsf{M}_\mathrm{c}^\# - \mathsf{M}_0) \cdot \Big(\sum_{n=2}^\infty e_n \mathsf{u}_n - \frac{1}{|U'|} \tilde{\zeta}_0 \overset{U'}{*} \sum_{n=2}^\infty e_n \mathsf{u}_n \Big), \mathsf{v}_1 \right)}_{=f(\boldsymbol{k})} \end{aligned} \tag{4.11}$$

Thus, we have the following integral equation,

$$h(\boldsymbol{k}) e_1(\boldsymbol{k}) + \frac{1}{|U'|} \int_{U'} e_1(\boldsymbol{k}') \tilde{\zeta}_0(\boldsymbol{k} - \boldsymbol{k}') g(\boldsymbol{k}, \boldsymbol{k}') \, \mathrm{d}v_{\boldsymbol{k}'} = f(\boldsymbol{k}) \tag{4.12}$$

which should be sufficient to determine $e_1(\boldsymbol{k})$, given that all other expansion coefficients have been determined, *i.e.*, $f(\boldsymbol{k})$ is a known function. Note that $h(\boldsymbol{k}) = \sigma_1(\boldsymbol{k}) - g(\boldsymbol{k}, \boldsymbol{k})$ and that both $\sigma_1(\boldsymbol{k})$ and $g(\boldsymbol{k}, \boldsymbol{k}')$ can be precomputed from the unit cell problem alone, *i.e.*, regardless of the shape of the finite array. This separates the problem into one computationally intensive problem for the cell, and one much less computationally intensive problem for the shape of the array.

Equation (4.12) is almost a Fredholm integral equation of the second kind, the big difference being that we cannot exclude the possibility that the function $h(\boldsymbol{k})$ may be zero for some $\boldsymbol{k}$. This is not straightforward to handle, and more analysis is required to understand the properties of this equation. Here, we restrict ourselves to providing some physical interpretation of this equation. In Appendix B, we also give an estimate of the norm of the integral operator.

From the singular value decomposition defined by (4.1) and (4.2), it is clear that $h(\boldsymbol{k}) = \sigma_1(\boldsymbol{k}) - (s(\mathsf{M}_\mathrm{c}^\# - \mathsf{M}_0) \cdot \mathsf{u}_1, \mathsf{v}_1) = (((\nabla + \mathrm{i}\boldsymbol{k}) \times \mathsf{J} + s\mathsf{M}_0) \cdot \mathsf{u}_1, \mathsf{v}_1)$. If there exists $\boldsymbol{k}$ such that $h(\boldsymbol{k}) = 0$, this means that the Maxwell operator corresponding to the surrounding medium, $(\nabla + \mathrm{i}\boldsymbol{k}) \times \mathsf{J} + s\mathsf{M}_0$, maps the singular vector u_1 into a space orthogonal to v_1. One such case is if u_1 corresponds to a freely propagating wave (eigenwave) in the *surrounding* medium, *i.e.*, $((\nabla + \mathrm{i}\boldsymbol{k}) \times \mathsf{J} + s\mathsf{M}_0) \cdot \mathsf{u}_1 = 0$. One case where this is the case is if the periodic medium $\mathsf{M}_\mathrm{c}^\#$ is a multiple of the surrounding medium M_0, *i.e.*, $\mathsf{M}_\mathrm{c}^\# = \kappa \mathsf{M}_0$ for some constant κ. However, this seems like a very unlikely case to occur, and in general the eigenwaves of the surrounding medium do not match the waves in the periodic medium.

5 Iterative scheme

We now return to equation (3.4), with the idea to formulate the iterative scheme

$$\tilde{\mathsf{e}} = \tilde{\mathsf{e}}^{(0)} + \tilde{\mathsf{e}}^{(1)} + \cdots \tag{5.1}$$

$$\tilde{\mathsf{e}}^{(0)} = ((\nabla + \mathrm{i}\boldsymbol{k}) \times \mathsf{J} + s\mathsf{M}_\mathrm{c}^\#)^{-1} \cdot (-\tilde{\mathsf{j}}) \tag{5.2}$$

$$\tilde{\mathsf{e}}^{(n+1)} = ((\nabla + \mathrm{i}\boldsymbol{k}) \times \mathsf{J} + s\mathsf{M}_\mathrm{c}^\#)^{-1} \cdot \left\{ s(\mathsf{M}_\mathrm{c}^\# - \mathsf{M}_0) \frac{1}{|U'|} \tilde{\zeta} \overset{U'}{*} \tilde{\mathsf{e}}^{(n)} \right\} \tag{5.3}$$

Using a moment method approach, the big computational load is paid in the computation of the impedance matrix representing the operator $(\nabla + \mathrm{i}\boldsymbol{k}) \times \mathsf{J} + s\mathsf{M}_\mathrm{c}^\#$ in this scheme. The extra computations due to the iterations do not cost much extra, except for the fact that we must discretize the entire reciprocal unit cell U', which means a new impedance matrix must be computed for each discretization point. However, this can easily be parallelized, and, most importantly, the computational work does not necessarily increase with the size of the structure.

Should eigenwaves be present, *i.e.*, the set Γ in (4.4) is nonempty and there exists $\boldsymbol{k} \in U'$ such that $\sigma_1(\boldsymbol{k}) = 0$, we split the field $\tilde{\mathsf{e}}$ into one corresponding to eigenwaves and one regular part according to

$$\tilde{\mathsf{e}} = \sum_{n=1}^{\infty} e_n \mathsf{u}_n = e_1 \mathsf{u}_1 + \sum_{n=2}^{\infty} e_n \mathsf{u}_n = e_1 \mathsf{u}_1 + \tilde{\mathsf{e}}_\mathrm{reg} \tag{5.4}$$

and modify the scheme to read

$$\tilde{\mathsf{e}}_{\mathrm{reg}}^{(0)} = (1-\mathrm{P}_0)((\nabla + \mathrm{i}\boldsymbol{k}) \times \mathsf{J} + s\mathsf{M}_{\mathrm{c}}^{\#})^{-1} \cdot (-\tilde{\mathsf{j}}) \tag{5.5}$$

$$\tilde{\mathsf{e}}_{\mathrm{reg}}^{(m+1)} = (1-\mathrm{P}_0)((\nabla + \mathrm{i}\boldsymbol{k}) \times \mathsf{J} + s\mathsf{M}_{\mathrm{c}}^{\#})^{-1} \cdot s(\mathsf{M}_{\mathrm{c}}^{\#} - \mathsf{M}_0) \cdot \frac{1}{|U'|}\tilde{\zeta} \overset{U'}{*} \tilde{\mathsf{e}}^{(m)} \tag{5.6}$$

$$h(\boldsymbol{k})e_1^{(m)}(\boldsymbol{k}) + \frac{1}{|U'|}\int_{U'} e_1^{(m)}(\boldsymbol{k}')\tilde{\zeta}'(\boldsymbol{k}-\boldsymbol{k}')g(\boldsymbol{k},\boldsymbol{k}')\,\mathrm{d}v_{\boldsymbol{k}'} = f^{(m)}(\boldsymbol{k}) \tag{5.7}$$

$$f^{(0)}(\boldsymbol{k}) = (-\tilde{\mathsf{j}}, \mathsf{v}_1) \tag{5.8}$$

$$f^{(m)}(\boldsymbol{k}) = (s(\mathsf{M}_{\mathrm{c}}^{\#} - \mathsf{M}_0) \cdot \frac{1}{|U'|}\tilde{\zeta} \overset{U'}{*} \tilde{\mathsf{e}}_{\mathrm{reg}}^{(m)}, \mathsf{v}_1), \quad m > 0 \tag{5.9}$$

where $\mathrm{P}_0 = (\cdot, \mathsf{v}_1)\mathsf{v}_1$ is the projection on the eigenwaves.

In both cases, the iteration corresponds to a Neumann series, and converges if the norm of the operator is less than one. We denote the L^2-norm over U by $\|f\|_{L^2(U)} = \int_U |f(\boldsymbol{x})|^2\,\mathrm{d}v_{\boldsymbol{x}}$, and the supremum norm over U and U' is denoted by $\|f\|_{L^\infty(U)} = \sup_{\boldsymbol{x}\in U}|f(\boldsymbol{x})|$ and $\|f\|_{L^\infty(U')} = \sup_{\boldsymbol{k}\in U'}|f(\boldsymbol{k})|$, respectively. The norm of a term in the iteration series is then

$$\begin{aligned}
\left\|\mathsf{e}^{(n+1)}\right\|^2 &= \frac{1}{|U'|}\int_{U'} \left\|\tilde{\mathsf{e}}^{(n+1)}\right\|_{L^2(U)}^2 \mathrm{d}v_{\boldsymbol{k}} \\
&= \frac{1}{|U'|}\int_{U'} \left\|((\nabla + \mathrm{i}\boldsymbol{k}) \times \mathsf{J} + s\mathsf{M}_{\mathrm{c}}^{\#})^{-1} \cdot \left\{ s(\mathsf{M}_{\mathrm{c}}^{\#} - \mathsf{M}_0)\frac{1}{|U'|}\tilde{\zeta} \overset{U'}{*} \tilde{\mathsf{e}}^{(n)} \right\}\right\|_{L^2(U)}^2 \mathrm{d}v_{\boldsymbol{k}} \\
&\le \frac{1}{|U'|}\int_{U'} \left\|((\nabla + \mathrm{i}\boldsymbol{k}) \times \mathsf{J} + s\mathsf{M}_{\mathrm{c}}^{\#})^{-1}\right\|^2 \left\|s(\mathsf{M}_{\mathrm{c}}^{\#} - \mathsf{M}_0)\right\|_{L^\infty(U)}^2 \left\|\frac{1}{|U'|}\tilde{\zeta} \overset{U'}{*} \tilde{\mathsf{e}}^{(n)}\right\|_{L^2(U)}^2 \mathrm{d}v_{\boldsymbol{k}} \\
&= \frac{\left\|s(\mathsf{M}_{\mathrm{c}}^{\#} - \mathsf{M}_0)\right\|_{L^\infty(U)}^2}{|U'|}\int_{U'} \frac{1}{\sigma_1^2}\left\|\frac{1}{|U'|}\tilde{\zeta} \overset{U'}{*} \tilde{\mathsf{e}}^{(n)}\right\|_{L^2(U)}^2 \mathrm{d}v_{\boldsymbol{k}} \\
&\le \left\|s(\mathsf{M}_{\mathrm{c}}^{\#} - \mathsf{M}_0)\right\|_{L^\infty(U)}^2 \left\|\frac{1}{\sigma_1^2}\right\|_{L^\infty(U')} \frac{1}{|U'|}\int_{U'} \left\|\frac{1}{|U'|}\tilde{\zeta} \overset{U'}{*} \tilde{\mathsf{e}}^{(n)}\right\|_{L^2(U)}^2 \mathrm{d}v_{\boldsymbol{k}}
\end{aligned} \tag{5.10}$$

where σ_1 is the smallest singular value of the operator $(\nabla + \mathrm{i}\boldsymbol{k}) \times \mathsf{J} + s\mathsf{M}_{\mathrm{c}}^{\#}$ and assumed nonzero for all $\boldsymbol{k} \in U'$. Should it happen that $\Gamma \neq \emptyset$, *i.e.*, eigenwaves are present and $\sigma_1(\boldsymbol{k}) = 0$ for $\boldsymbol{k} \in \Gamma$, the above estimate is valid for the regular part of the solution $\tilde{\mathsf{e}}_{\mathrm{reg}}$, with σ_1 replaced by σ_2. The expansion coefficient $e_1(\boldsymbol{k})$ is then calculated as the solution to the integral equation (4.12), and must be estimated in terms of $f(\boldsymbol{k})$. At the present level of understanding, explicit estimates are not possible, and we have to conjecture that this can be done.

In the next section we show that under reasonable conditions on $\tilde{\mathsf{e}}^{(n)}$, we can prove an estimate of the sort

$$\frac{1}{|U'|}\int_{U'} \left\|\frac{1}{|U'|}\tilde{\zeta} \overset{U'}{*} \tilde{\mathsf{e}}^{(n)}\right\|_{L^2(U)}^2 \mathrm{d}v_{\boldsymbol{k}} \le C_N \left\|\mathsf{e}^{(n)}\right\|^2 \tag{5.11}$$

where the constant C_N should be $\mathrm{o}(1/N)$, where N is the number of unit cells in the finite structure.

6 Convergence of the iterative scheme

In this section we show that the convolution with the Bloch amplitude of the window function tends to zero for functions that are sufficiently smooth in $\boldsymbol{k}$. We write

$$\left[\frac{1}{|U'|}\tilde{\zeta} \overset{U'}{*} \tilde{f}\right](\boldsymbol{x},\boldsymbol{k}) = \frac{1}{|U'|}\int_{U'}\left(\sum_{\boldsymbol{n}\notin I} \mathrm{e}^{-\mathrm{i}\boldsymbol{k}'\cdot(\boldsymbol{x}+\boldsymbol{x}_{\boldsymbol{n}})}\right)\tilde{f}(\boldsymbol{x},\boldsymbol{k}-\boldsymbol{k}')\,\mathrm{d}v_{\boldsymbol{k}'} \tag{6.1}$$

Since $\mathrm{e}^{\mathrm{i}\boldsymbol{k}\cdot\boldsymbol{x}}\tilde{f}(\boldsymbol{x},\boldsymbol{k})$ is U'-periodic in $\boldsymbol{k}$, we rewrite this as

$$\left[\frac{1}{|U'|}\tilde{\zeta} \overset{U'}{*} \tilde{f}\right](\boldsymbol{x},\boldsymbol{k}) = \frac{\mathrm{e}^{-\mathrm{i}\boldsymbol{k}\cdot\boldsymbol{x}}}{|U'|}\int_{U'}\left(\sum_{\boldsymbol{n}\notin I} \mathrm{e}^{-\mathrm{i}\boldsymbol{k}'\cdot\boldsymbol{x}_{\boldsymbol{n}}}\right)\mathrm{e}^{\mathrm{i}(\boldsymbol{k}-\boldsymbol{k}')\cdot\boldsymbol{x}}\tilde{f}(\boldsymbol{x},\boldsymbol{k}-\boldsymbol{k}')\,\mathrm{d}v_{\boldsymbol{k}'} \tag{6.2}$$

which permits us to do the integration by parts necessary for the following computations, which are classical in estimating linear phase contributions in a stationary phase analysis of oscillating integrals, see for instance [8, p. 210]. For the moment, we assume $\tilde{f}$ is smooth enough for the calculations to be valid. Thus, we have

$$\begin{aligned}
&\frac{\mathrm{e}^{-\mathrm{i}\boldsymbol{k}\cdot\boldsymbol{x}}}{|U'|}\int_{U'}\left(\sum_{\boldsymbol{n}\notin I} \mathrm{e}^{-\mathrm{i}\boldsymbol{k}'\cdot\boldsymbol{x}_{\boldsymbol{n}}}\right)\mathrm{e}^{\mathrm{i}(\boldsymbol{k}-\boldsymbol{k}')\cdot\boldsymbol{x}}\tilde{f}(\boldsymbol{x},\boldsymbol{k}-\boldsymbol{k}')\,\mathrm{d}v_{\boldsymbol{k}'}\\
&\quad= \frac{\mathrm{e}^{-\mathrm{i}\boldsymbol{k}\cdot\boldsymbol{x}}}{|U'|}\sum_{\boldsymbol{n}\notin I}\frac{1}{(-\mathrm{i}\boldsymbol{x}_{\boldsymbol{n}})^{\alpha}}\int_{U'}\left(\frac{\partial^{|\alpha|}}{\partial(\boldsymbol{k}')^{\alpha}}\mathrm{e}^{-\mathrm{i}\boldsymbol{k}'\cdot\boldsymbol{x}_{\boldsymbol{n}}}\right)\mathrm{e}^{\mathrm{i}(\boldsymbol{k}-\boldsymbol{k}')\cdot\boldsymbol{x}}\tilde{f}(\boldsymbol{x},\boldsymbol{k}-\boldsymbol{k}')\,\mathrm{d}v_{\boldsymbol{k}'}\\
&\quad= \frac{\mathrm{e}^{-\mathrm{i}\boldsymbol{k}\cdot\boldsymbol{x}}}{|U'|}\sum_{\boldsymbol{n}\notin I}\frac{1}{(\mathrm{i}\boldsymbol{x}_{\boldsymbol{n}})^{\alpha}}\int_{U'}\mathrm{e}^{-\mathrm{i}\boldsymbol{k}'\cdot\boldsymbol{x}_{\boldsymbol{n}}}\frac{\partial^{|\alpha|}}{\partial(\boldsymbol{k}')^{\alpha}}\left(\mathrm{e}^{\mathrm{i}(\boldsymbol{k}-\boldsymbol{k}')\cdot\boldsymbol{x}}\tilde{f}(\boldsymbol{x},\boldsymbol{k}-\boldsymbol{k}')\right)\mathrm{d}v_{\boldsymbol{k}'}
\end{aligned} \tag{6.3}$$

where we use multiindex notation for the derivatives with respect to $\boldsymbol{k}'$, *i.e.*,

$$\frac{\partial^{|\alpha|}}{\partial(\boldsymbol{k}')^{\alpha}} = \frac{\partial^{|\alpha|}}{\partial(k_1')^{\alpha_1}\partial(k_2')^{\alpha_2}\partial(k_3')^{\alpha_3}} \quad\text{and}\quad \frac{1}{(\mathrm{i}\boldsymbol{x}_{\boldsymbol{n}})^{\alpha}} = \frac{1}{(\mathrm{i}x_{\boldsymbol{n}1})^{\alpha_1}(\mathrm{i}x_{\boldsymbol{n}2})^{\alpha_2}(\mathrm{i}x_{\boldsymbol{n}3})^{\alpha_3}} \tag{6.4}$$

where $|\alpha| = \alpha_1+\alpha_2+\alpha_3$ (if the structure is periodic in only one or two dimensions, we of course only have α_1 or $\alpha_{1,2}$ nonzero). We write

$$\begin{aligned}
\left|\left[\frac{1}{|U'|}\tilde{\zeta} \overset{U'}{*} \tilde{f}\right](\boldsymbol{x},\boldsymbol{k})\right| &= \left|\frac{\mathrm{e}^{-\mathrm{i}\boldsymbol{k}\cdot\boldsymbol{x}}}{|U'|}\sum_{\boldsymbol{n}\notin I}\frac{1}{(\mathrm{i}\boldsymbol{x}_{\boldsymbol{n}})^{\alpha}}\left[\mathrm{e}^{-\mathrm{i}\boldsymbol{k}\cdot\boldsymbol{x}_{\boldsymbol{n}}} \overset{U'}{*} \frac{\partial^{|\alpha|}}{\partial(\boldsymbol{k})^{\alpha}}\left(\mathrm{e}^{\mathrm{i}\boldsymbol{k}\cdot\boldsymbol{x}}\tilde{f}\right)\right](\boldsymbol{x},\boldsymbol{k})\right|\\
&\le \frac{1}{|U'|}\sum_{\boldsymbol{n}\notin I}\frac{1}{|\boldsymbol{x}_{\boldsymbol{n}}^{\alpha}|}\left|\left[\mathrm{e}^{-\mathrm{i}\boldsymbol{k}\cdot\boldsymbol{x}_{\boldsymbol{n}}} \overset{U'}{*} \frac{\partial^{|\alpha|}}{\partial(\boldsymbol{k})^{\alpha}}\left(\mathrm{e}^{\mathrm{i}\boldsymbol{k}\cdot\boldsymbol{x}}\tilde{f}\right)\right](\boldsymbol{x},\boldsymbol{k})\right|\\
&\le \frac{1}{|U'|}\sum_{\boldsymbol{n}\notin I}\frac{1}{|\boldsymbol{x}_{\boldsymbol{n}}^{\alpha}|}\left\|\mathrm{e}^{-\mathrm{i}\boldsymbol{k}\cdot\boldsymbol{x}_{\boldsymbol{n}}}\right\|_{L^2(U')}\left\|\frac{\partial^{|\alpha|}}{\partial(\boldsymbol{k})^{\alpha}}\left(\mathrm{e}^{\mathrm{i}\boldsymbol{k}\cdot\boldsymbol{x}}\tilde{f}\right)\right\|_{L^2(U')}
\end{aligned} \tag{6.5}$$

where we used the general estimate $|f * g| \leq \|f\|_{L^2} \|g\|_{L^2}$ for convolutions [12, p. 116]. Since $\left\|\mathrm{e}^{-\mathrm{i}\boldsymbol{k}\cdot\boldsymbol{x}}\right\|_{L^2(U')} = (\int_{U'} |\mathrm{e}^{-\mathrm{i}\boldsymbol{k}\cdot\boldsymbol{x}}|^2 \,\mathrm{d}v_{\boldsymbol{k}})^{1/2} = |U'|^{1/2}$, we have

$$\begin{aligned}\frac{1}{|U'|}\int_{U'}\left\|\frac{1}{|U'|}\tilde{\zeta} \overset{U'}{*} \tilde{f}\right\|^2_{L^2(U)} \mathrm{d}v_{\boldsymbol{k}} &= \frac{1}{|U'|}\int_{U'}\int_{U}\left|\frac{1}{|U'|}\tilde{\zeta} \overset{U'}{*} \tilde{f}\right|^2 \mathrm{d}v_{\boldsymbol{x}}\,\mathrm{d}v_{\boldsymbol{k}} \\ &\leq \left(\sum_{\boldsymbol{n}\notin I}\frac{1}{|\boldsymbol{x}_{\boldsymbol{n}}^{\alpha}|}\right)^2 \frac{1}{|U'|}\int_{U'}\int_{U}\left|\frac{\partial^{|\alpha|}}{\partial \boldsymbol{k}^{\alpha}}\left(\mathrm{e}^{\mathrm{i}\boldsymbol{k}\cdot\boldsymbol{x}}\tilde{f}(\boldsymbol{x},\boldsymbol{k})\right)\right|^2 \mathrm{d}v_{\boldsymbol{x}}\,\mathrm{d}v_{\boldsymbol{k}} \quad (6.6)\end{aligned}$$

Assuming that $\tilde{f}$ is sufficiently smooth in $\boldsymbol{k}$ to allow

$$\frac{1}{|U'|}\int_{U'}\int_{U}\left|\frac{\partial^{|\alpha|}}{\partial \boldsymbol{k}^{\alpha}}\left(\mathrm{e}^{\mathrm{i}\boldsymbol{k}\cdot\boldsymbol{x}}\tilde{f}(\boldsymbol{x},\boldsymbol{k})\right)\right|^2 \mathrm{d}v_{\boldsymbol{k}} \leq C_f \|f\|^2 \quad (6.7)$$

we combine (6.6) with (5.10) to form

$$\left\|\mathsf{e}^{(n+1)}\right\|^2 \leq \left\|s(\mathsf{M}_{\mathrm{c}}^{\#} - \mathsf{M}_0)\right\|^2_{L^\infty(U)} \left\|\frac{1}{\sigma_1}\right\|^2_{L^\infty(U')} \left(\sum_{\boldsymbol{n}\notin I}\frac{1}{|\boldsymbol{x}_{\boldsymbol{n}}^{\alpha}|}\right)^2 C_{\mathsf{e}^{(n)}} \left\|\mathsf{e}^{(n)}\right\|^2 \quad (6.8)$$

We now conjecture that there exists a C such that for all n we have $C_{\mathsf{e}^{(n)}} \leq C$, *i.e.*, the sequence $\{\mathsf{e}^{(n)}\}_{n=0}^{\infty}$ is uniformly bounded in a suitable Sobolev space, with $|\alpha|$ weak derivatives with respect to $\boldsymbol{k}$. The multiindex α must be large enough to guarantee

$$\sum_{\boldsymbol{n}\notin I}\frac{1}{|\boldsymbol{x}_{\boldsymbol{n}}^{\alpha}|} = \mathrm{o}(1/N) \quad (6.9)$$

which roughly requires $|\alpha| > d$, where d is the number of lattice dimensions for the periodic structure. Typically, the series is of the same order as its first term $1/|\boldsymbol{x}_N|^{|\alpha|} = 1/R^{|\alpha|}$, where R is the radius of the structure. From this result we see that the iterative scheme can be guaranteed to converge if there are sufficiently many unit cells in the finite periodic structure, *i.e.*, N is large enough to guarantee

$$\left\|s(\mathsf{M}_{\mathrm{c}}^{\#} - \mathsf{M}_0)\right\|^2_{L^\infty(U)} \left\|\frac{1}{\sigma_1}\right\|^2_{L^\infty(U')} \left(\sum_{\boldsymbol{n}\notin I}\frac{1}{|\boldsymbol{x}_{\boldsymbol{n}}^{\alpha}|}\right)^2 C < 1 \quad (6.10)$$

which is the requirement for the Neumann series corresponding to the iterative scheme to converge. Once again, the case where eigenwaves are present must be treated separately, taking into account the integral equation (4.12).

7 Regularity of solutions with respect to the wave vector

In the previous section we showed that the iterative scheme converges for a large enough structure if we can find uniform bounds on the derivatives of $\mathsf{e}^{(n)}$ with respect

to $\boldsymbol{k}$. To prove that this is the case is a formidable task, but we present here an argument that at least makes it plausible.

Let's return to the zeroth order equation

$$((\nabla + \mathrm{i}\boldsymbol{k}) \times \mathsf{J} + s\mathsf{M}_{\mathrm{c}}^{\#}) \cdot \tilde{\mathsf{e}}^{(0)} = -\tilde{\mathsf{j}} \tag{7.1}$$

From this equation it seems reasonable to expect as much regularity in $\tilde{\mathsf{e}}^{(0)}$ with respect to $\boldsymbol{k}$ as there is in $\tilde{\mathsf{j}}$, since the operator $(\nabla + \mathrm{i}\boldsymbol{k}) \times \mathsf{J} + s\mathsf{M}_{\mathrm{c}}^{\#}$ is analytical in $\boldsymbol{k}$. The only point where this may not be valid is when $\boldsymbol{k}$ corresponds to the existence of eigenmodes, or resonances, in the structure.

To see this explicitly, we differentiate the above equation with respect to the i:th component of $\boldsymbol{k}$, $i = 1, 2, 3$, which provides

$$((\nabla + \mathrm{i}\boldsymbol{k}) \times \mathsf{J} + s\mathsf{M}_{\mathrm{c}}^{\#}) \cdot \partial_{k_i}\tilde{\mathsf{e}}^{(0)} + \mathrm{i}\hat{\boldsymbol{x}}_i \times \mathsf{J} \cdot \tilde{\mathsf{e}}^{(0)} = -\partial_{k_i}\tilde{\mathsf{j}} \tag{7.2}$$

or

$$\partial_{k_i}\tilde{\mathsf{e}}^{(0)} = ((\nabla + \mathrm{i}\boldsymbol{k}) \times \mathsf{J} + s\mathsf{M}_{\mathrm{c}}^{\#})^{-1} \cdot \left[-\mathrm{i}\hat{\boldsymbol{x}}_i \times \mathsf{J} \cdot \tilde{\mathsf{e}}^{(0)} - \partial_{k_i}\tilde{\mathsf{j}}\right] \tag{7.3}$$

This demonstrates that the derivatives of $\tilde{\mathsf{e}}_0$ with respect to $\boldsymbol{k}$ can be bounded by lower order derivatives of $\tilde{\mathsf{e}}_0$ and the same order of derivatives of $\tilde{\mathsf{j}}$, provided $((\nabla + \mathrm{i}\boldsymbol{k}) \times \mathsf{J} + s\mathsf{M}_{\mathrm{c}}^{\#})^{-1}$ is a bounded operator. This only fails for $\boldsymbol{k}$ such that the null space of $(\nabla + \mathrm{i}\boldsymbol{k}) \times \mathsf{J} + s\mathsf{M}_{\mathrm{c}}^{\#}$ is nonempty, *i.e.*, for eigenwaves, which would have to be treated through the integral equation (4.12).

The remaining question is how regular $\tilde{\mathsf{e}}^{(n+1)}$ is in terms of the regularity of $\tilde{\mathsf{e}}^{(n)}$. We then have the equation

$$((\nabla + \mathrm{i}\boldsymbol{k}) \times \mathsf{J} + s\mathsf{M}_{\mathrm{c}}^{\#}) \cdot \tilde{\mathsf{e}}^{(n+1)} = s(\mathsf{M}_{\mathrm{c}}^{\#} - \mathsf{M}_0) \cdot \frac{1}{|U'|}\tilde{\zeta} \overset{U'}{*} \tilde{\mathsf{e}}^{(n)} \tag{7.4}$$

Since the convolution operation commutes with ∂_{k_i}, this means the smoothness with respect to $\boldsymbol{k}$ carries over to all terms in the series $\tilde{\mathsf{e}}_1$, $\tilde{\mathsf{e}}_2$ etc. Once again, exceptions occur for $\boldsymbol{k}$:s corresponding to eigenwaves.

The calculations in this section show that the constant $C_{\mathsf{e}^{(n)}}$ is essentially given by $\left\|((\nabla + \mathrm{i}\boldsymbol{k}) \times \mathsf{J} + s\mathsf{M}_{\mathrm{c}}^{\#})^{-1}\right\|^2 \leq \|1/\sigma_1\|^2_{L^\infty(U')}$, which is independent of n and thus can be uniformly bounded.

8 A brief outline of implementation possibilities

When formulating the algorithm presented in this paper, we have had in mind the possibility of using a moment method code like Randolph in the Swedish code GEMS, General ElectroMagnetic Solvers. This code has recently been augmented with the possibility of using periodic boundary conditions, and should be ideal to compute the solution to the unit cell problems necessary.

In the moment method, the computationally intensive part is to compute the impedance matrix. Once this is done, the problem can be solved rather quickly for arbitrary sources. The impedance matrix must be recalculated for each frequency ω and each wave vector $\boldsymbol{k} \in U'$. Thus, the number of impedance matrices to compute

depends heavily on the dimension of U'. Since we only need a partial singular value decomposition, to obtain the first singular value and its vectors, the computational overhead due to the SVD should not pose a big problem.

A straightforward way of implementing the algorithm would be the following, where we only consider the calculation of the result for a single frequency. We assume we have access to a cluster with a large number of nodes, numbered from 0 to N.

1. Let nodes 1–N calculate and store the impedance matrix corresponding to a fixed $\boldsymbol{k} \in U'$, *i.e.*, each node represents a discretization point in U'.

2. Let nodes 1–N perform a partial singular value decomposition of their respective impedance matrix to extract σ_1, u_1 and v_1.

3. Let node 0 compute the factors $h(\boldsymbol{k})$ and $g(\boldsymbol{k}, \boldsymbol{k}')$ in the integral equation (4.12) from the SVD results.

4. Let node 0 compute the right hand side from the previous solution vectors and distribute it to nodes 1–N.

5. Let each node 1–N compute its new solution vector.

6. Let node 0 collect the solution vectors from each of the nodes 1–N, go to 4.

Thus, the computational complexity is increased by roughly a factor corresponding to the number of discretization points in U'. In principle, this does not increase with the number of elements used in the periodic structure, but since $\tilde{\zeta}_0$ is rapidly oscillating for large periodic structures, some additional care must be taken to ensure that the convolution integral is performed satisfactorily. One possibility is to perform the convolution by a forward FFT, followed by multiplication of the window function in the spatial domain and an inverse FFT. We note that depending on the number of discretization points in U', the algorithm may not be competitive until a very large number of elements are employed.

9 Conclusions

We have demonstrated an algorithm which is able to treat very large finite periodic structures using methods based on infinite periodicity. The algorithm is based on taking care of the large scale variations through the Floquet-Bloch wave vector $\boldsymbol{k}$, which is restricted to the first Brillouin zone U', *i.e.*, a bounded region.

The algorithm is shown to converge if the periodic structure is large enough, but at present it is difficult to give an accurate estimate on how large it has to be. Even if only a few iterations may be sufficient to produce acceptable information on the influence of the finiteness of the structure, we wish to point out that compared to the work spent at computing the impedance matrices, the iterations are practically for free. In particular, the zeroth iteration only involves a convolution with the impressed currents $\tilde{\mathsf{j}}$, corresponding to standard windowing techniques.

Problems occur in the analysis if eigenwaves are present, *i.e.*, the infinite periodic structure allows the free propagation of undamped waves. In the case of an array antenna, this corresponds to surface waves. These waves can be very precisely characterized, and constitute only a subset of very low dimension to the solution space. We have derived an integral equation which can be used to determine this solution, where essentially the entire finite periodic structure is studied at once.

Many of the estimates in this paper are rough, with the only goal to demonstrate that it is likely the algorithm works. To give sharper estimates of the validity range and convergence rate of the algorithm, more rigorous calculations are necessary.

The requirements of many other algorithms targeted at large structures grow with the size of the structure. Since the present algorithm is based on the Bloch amplitude of the window function $\tilde{\zeta}$, which approaches the Dirac distribution as the size of the structure increases, it might even need *less* discretization in U' as the structure grows. However, this is a complicated issue since the function $\tilde{\zeta}$ is rapidly oscillating for a large structure, and certainly requires more analysis.

The results in this paper can be applied to any finite periodic structure, *i.e.*, finite phased array antennas, finite frequency selective surfaces (FSS), or finite photonic bandgap crystals (PBG). Some interesting further work may be to investigate the low frequency limit of the algorithm to discover the proper effective boundary conditions of a finite material with periodic microscopic structure. This may or may not lead to the introduction of boundary layer theories in effective models of the periodic structure, or it may provide guidelines on how to suppress surface waves in array antennas as in [11].

10 Acknowledgements

The work reported in this paper was financially supported by the Swedish Defence Administration (FMV). The author thanks Gerhard Kristensson, Mats Gustafsson and Anders Karlsson at the Department of Electroscience, Lund University, for many constructive discussions regarding the results in this paper.

Appendix A Some computational rules for the Floquet-Bloch representation

In this appendix we summarize some useful rules for doing calculations involving the Floquet-Bloch representation of fields.

To start with, the Dirac delta function can be represented as [21]

$$\frac{1}{|U'|}\sum_{\boldsymbol{n}\in\mathbb{Z}^3} \mathrm{e}^{\mathrm{i}\boldsymbol{k}\cdot\boldsymbol{x}_{\boldsymbol{n}}} = \delta(\boldsymbol{k}) \tag{A.1}$$

We use this representation to prove a number of results in this section. Now let

$f \in L^2(\mathbb{R}^3)$, *i.e.*, f is square integrable over $\mathbb{R}^3$. It can then be represented by

$$f(\boldsymbol{x}) = \frac{1}{|U'|} \int_{U'} \mathrm{e}^{\mathrm{i}\boldsymbol{k}\cdot\boldsymbol{x}} \tilde{f}(\boldsymbol{x}, \boldsymbol{k}) \, \mathrm{d}v_{\boldsymbol{k}} \tag{A.2}$$

where the Bloch amplitude $\tilde{f}$ is given by

$$\tilde{f}(\boldsymbol{x}, \boldsymbol{k}) = \frac{1}{|U|} \sum_{\boldsymbol{n}\in\mathbb{Z}^3} \mathrm{e}^{\mathrm{i}\boldsymbol{k}_{\boldsymbol{n}}\cdot\boldsymbol{x}} \hat{f}(\boldsymbol{k} + \boldsymbol{k}_{\boldsymbol{n}}) = \sum_{\boldsymbol{n}\in\mathbb{Z}^3} \mathrm{e}^{-\mathrm{i}\boldsymbol{k}\cdot(\boldsymbol{x}+\boldsymbol{x}_{\boldsymbol{n}})} f(\boldsymbol{x} + \boldsymbol{x}_{\boldsymbol{n}}) \tag{A.3}$$

and $\hat{f}$ is the Fourier transform

$$\hat{f}(\boldsymbol{k}) = \int_{\mathbb{R}^3} \mathrm{e}^{-\mathrm{i}\boldsymbol{k}\cdot\boldsymbol{x}} f(\boldsymbol{x}) \, \mathrm{d}v_{\boldsymbol{x}} \tag{A.4}$$

From (A.3) it is seen that the **mean value** of the Bloch amplitude is

$$\langle \tilde{f}(\cdot, \boldsymbol{k}) \rangle = \hat{f}(\boldsymbol{k}), \quad \boldsymbol{k} \in U' \tag{A.5}$$

and the Bloch amplitude is periodic in $\boldsymbol{x}$ and pseudoperiodic in $\boldsymbol{k}$, *i.e.*,

$$\tilde{f}(\boldsymbol{x} + \boldsymbol{x}_{\boldsymbol{n}}, \boldsymbol{k}) = \tilde{f}(\boldsymbol{x}, \boldsymbol{k}) \quad \text{and} \quad \tilde{f}(\boldsymbol{x}, \boldsymbol{k} + \boldsymbol{k}_{\boldsymbol{n}}) = \mathrm{e}^{-\mathrm{i}\boldsymbol{k}_{\boldsymbol{n}}\cdot\boldsymbol{x}} \tilde{f}(\boldsymbol{x}, \boldsymbol{k}) \tag{A.6}$$

The norm of f can be expressed in three different ways

$$\underbrace{\int_{\mathbb{R}^3} |f(\boldsymbol{x})|^2 \, \mathrm{d}v_{\boldsymbol{x}}}_{\|f\|^2} = \underbrace{\frac{1}{(2\pi)^3} \int_{\mathbb{R}^3} |\hat{f}(\boldsymbol{k})|^2 \, \mathrm{d}v_{\boldsymbol{k}}}_{(2\pi)^{-3}\left\|\hat{f}\right\|^2} = \underbrace{\frac{1}{|U'|} \int_{U'} \int_{U} |\tilde{f}(\boldsymbol{x}, \boldsymbol{k})|^2 \, \mathrm{d}v_{\boldsymbol{x}} \, \mathrm{d}v_{\boldsymbol{k}}}_{|U'|^{-1}\int_{U'}\left\|\tilde{f}(\cdot,\boldsymbol{k})\right\|^2 \mathrm{d}v_{\boldsymbol{k}}} \tag{A.7}$$

which is seen from

$$\begin{aligned}
\int_{\mathbb{R}^3} |f(\boldsymbol{x})|^2 \, \mathrm{d}v_{\boldsymbol{x}} &= \int_{\mathbb{R}^3} \left[\frac{1}{|U'|} \int_{U'} \mathrm{e}^{\mathrm{i}\boldsymbol{k}'\cdot\boldsymbol{x}} \tilde{f}(\boldsymbol{x}, \boldsymbol{k}') \, \mathrm{d}v_{\boldsymbol{k}'} \right]^* \left[\frac{1}{|U'|} \int_{U'} \mathrm{e}^{\mathrm{i}\boldsymbol{k}\cdot\boldsymbol{x}} \tilde{f}(\boldsymbol{x}, \boldsymbol{k}) \, \mathrm{d}v_{\boldsymbol{k}} \right] \mathrm{d}v_{\boldsymbol{x}} \\
&= \sum_{\boldsymbol{n}\in\mathbb{Z}^3} \int_{U} \frac{1}{|U'|^2} \int_{U'} \int_{U'} \mathrm{e}^{\mathrm{i}(\boldsymbol{k}-\boldsymbol{k}')\cdot\boldsymbol{x}_{\boldsymbol{n}}} \mathrm{e}^{\mathrm{i}(\boldsymbol{k}-\boldsymbol{k}')\cdot\boldsymbol{x}} [\tilde{f}(\boldsymbol{x}, \boldsymbol{k}')]^* \tilde{f}(\boldsymbol{x}, \boldsymbol{k}) \, \mathrm{d}v_{\boldsymbol{k}} \, \mathrm{d}v_{\boldsymbol{k}'} \, \mathrm{d}v_{\boldsymbol{x}} \\
&= \frac{1}{|U'|} \int_{U'} \int_{U} |\tilde{f}(\boldsymbol{x}, \boldsymbol{k})|^2 \, \mathrm{d}v_{\boldsymbol{x}} \, \mathrm{d}v_{\boldsymbol{k}}
\end{aligned} \tag{A.8}$$

where we used the representation of the delta function (A.1).

The nabla operator becomes a shifted nabla operator for the Bloch amplitude

$$\nabla f(\boldsymbol{x}) = \frac{1}{|U'|} \int_{U'} \mathrm{e}^{\mathrm{i}\boldsymbol{k}\cdot\boldsymbol{x}} (\nabla + \mathrm{i}\boldsymbol{k}) \tilde{f}(\boldsymbol{x}, \boldsymbol{k}) \, \mathrm{d}v_{\boldsymbol{x}} \tag{A.9}$$

The convolution between two functions can be expressed as a convolution between the Bloch amplitudes

$$
\begin{aligned}
[f * g](\boldsymbol{x}) &= \int_{\mathbb{R}^3} f(\boldsymbol{x}')g(\boldsymbol{x}-\boldsymbol{x}')\,\mathrm{d}v_{\boldsymbol{x}'} \\
&= \int_{\mathbb{R}^3} \left[\frac{1}{|U'|}\int_{U'} \mathrm{e}^{\mathrm{i}\boldsymbol{k}'\cdot\boldsymbol{x}'}\tilde{f}(\boldsymbol{x}',\boldsymbol{k}')\,\mathrm{d}v_{\boldsymbol{k}'}\right]\left[\frac{1}{|U'|}\int_{U'} \mathrm{e}^{\mathrm{i}\boldsymbol{k}\cdot(\boldsymbol{x}-\boldsymbol{x}')}\tilde{g}(\boldsymbol{x}-\boldsymbol{x}',\boldsymbol{k})\,\mathrm{d}v_{\boldsymbol{k}}\right]\mathrm{d}v_{\boldsymbol{x}'} \\
&= \sum_{\boldsymbol{n}\in\mathbb{Z}^3}\int_U \frac{1}{|U'|^2}\int_{U'}\int_{U'} \mathrm{e}^{\mathrm{i}(\boldsymbol{k}'-\boldsymbol{k})\cdot\boldsymbol{x}_{\boldsymbol{n}}}\mathrm{e}^{\mathrm{i}(\boldsymbol{k}'-\boldsymbol{k})\cdot\boldsymbol{x}'}\mathrm{e}^{\mathrm{i}\boldsymbol{k}\cdot\boldsymbol{x}}\tilde{f}(\boldsymbol{x}',\boldsymbol{k}')\tilde{g}(\boldsymbol{x}-\boldsymbol{x}',\boldsymbol{k})\,\mathrm{d}v_{\boldsymbol{k}}\,\mathrm{d}v_{\boldsymbol{k}'}\,\mathrm{d}v_{\boldsymbol{x}'} \\
&= \frac{1}{|U'|}\int_{U'} \mathrm{e}^{\mathrm{i}\boldsymbol{k}\cdot\boldsymbol{x}}\int_U \tilde{f}(\boldsymbol{x}',\boldsymbol{k})\tilde{g}(\boldsymbol{x}-\boldsymbol{x}',\boldsymbol{k})\,\mathrm{d}v_{\boldsymbol{x}'}\,\mathrm{d}v_{\boldsymbol{k}} \\
&= \frac{1}{|U'|}\int_{U'} \mathrm{e}^{\mathrm{i}\boldsymbol{k}\cdot\boldsymbol{x}}[\tilde{f} \overset{U}{*} \tilde{g}](\boldsymbol{x},\boldsymbol{k})\,\mathrm{d}v_{\boldsymbol{k}} \qquad \text{(A.10)}
\end{aligned}
$$

where we once again used (A.1), and use the notation $\overset{U}{*}$ to denote convolution over the unit cell U.

The product between two functions can be studied for two cases. First, let g be a periodic function, *i.e.*, $g(\boldsymbol{x}+\boldsymbol{x}_{\boldsymbol{n}}) = g(\boldsymbol{x})$. It is clear that $g \notin L^2(\mathbb{R}^3)$, but with $g \in L^\infty(U)$ and $f \in L^2(\mathbb{R}^3)$ we still have $fg \in L^2(\mathbb{R}^3)$. This implies that the Bloch amplitude is

$$
[\widetilde{fg}](\boldsymbol{x},\boldsymbol{k}) = \sum_{\boldsymbol{n}\in\mathbb{Z}^3} \mathrm{e}^{-\mathrm{i}\boldsymbol{k}\cdot(\boldsymbol{x}+\boldsymbol{x}_{\boldsymbol{n}})} f(\boldsymbol{x}+\boldsymbol{x}_{\boldsymbol{n}})g(\boldsymbol{x}+\boldsymbol{x}_{\boldsymbol{n}}) = \tilde{f}(\boldsymbol{x},\boldsymbol{k})g(\boldsymbol{x}) \qquad \text{(A.11)}
$$

or

$$
f(\boldsymbol{x})g(\boldsymbol{x}) = \frac{1}{|U'|}\int_{U'} \mathrm{e}^{\mathrm{i}\boldsymbol{k}\cdot\boldsymbol{x}}\tilde{f}(\boldsymbol{x},\boldsymbol{k})g(\boldsymbol{x})\,\mathrm{d}v_{\boldsymbol{k}} \qquad \text{(A.12)}
$$

Next, let $g \in L^\infty(\mathbb{R}^3)$ and $f \in L^2(\mathbb{R}^3)$, which means $fg \in L^2(\mathbb{R}^3)$. Even though $g \in L^\infty(\mathbb{R}^3)$ does not guarantee the existence of the Fourier transform $\hat{g}$ in a proper manner, we still make the formal calculation

$$
\begin{aligned}
[\widetilde{fg}](\boldsymbol{x},\boldsymbol{k}) &= \frac{1}{|U|}\sum_{\boldsymbol{n}\in\mathbb{Z}^3} \mathrm{e}^{\mathrm{i}\boldsymbol{k}_{\boldsymbol{n}}\cdot\boldsymbol{x}}[\widehat{fg}](\boldsymbol{k}+\boldsymbol{k}_{\boldsymbol{n}}) = \frac{1}{|U|}\sum_{\boldsymbol{n}\in\mathbb{Z}^3} \mathrm{e}^{\mathrm{i}\boldsymbol{k}_{\boldsymbol{n}}\cdot\boldsymbol{x}}\frac{1}{(2\pi)^3}[\hat{f} * \hat{g}](\boldsymbol{k}+\boldsymbol{k}_{\boldsymbol{n}}) \\
&= \frac{1}{|U|(2\pi)^3}\sum_{\boldsymbol{n}\in\mathbb{Z}^3} \mathrm{e}^{\mathrm{i}\boldsymbol{k}_{\boldsymbol{n}}\cdot\boldsymbol{x}}\int_{\mathbb{R}^3} \hat{f}(\boldsymbol{k}')\hat{g}(\boldsymbol{k}+\boldsymbol{k}_{\boldsymbol{n}}-\boldsymbol{k}')\,\mathrm{d}v_{\boldsymbol{k}'} \\
&= \frac{1}{|U|(2\pi)^3}\sum_{\boldsymbol{n}\in\mathbb{Z}^3} \mathrm{e}^{\mathrm{i}\boldsymbol{k}_{\boldsymbol{n}}\cdot\boldsymbol{x}}\sum_{\boldsymbol{n}'\in\mathbb{Z}^3}\int_{U'} \hat{f}(\boldsymbol{k}'+\boldsymbol{k}_{\boldsymbol{n}'})\hat{g}(\boldsymbol{k}+\boldsymbol{k}_{\boldsymbol{n}}-\boldsymbol{k}'-\boldsymbol{k}_{\boldsymbol{n}'})\,\mathrm{d}v_{\boldsymbol{k}'} \\
&= \frac{1}{(2\pi)^3}\sum_{\boldsymbol{n}'\in\mathbb{Z}^3}\int_{U'} \hat{f}(\boldsymbol{k}'+\boldsymbol{k}_{\boldsymbol{n}'})\tilde{g}(\boldsymbol{x},\boldsymbol{k}-\boldsymbol{k}'-\boldsymbol{k}_{\boldsymbol{n}'})\,\mathrm{d}v_{\boldsymbol{k}'} \\
&= \frac{1}{(2\pi)^3}\sum_{\boldsymbol{n}'\in\mathbb{Z}^3}\int_{U'} \hat{f}(\boldsymbol{k}'+\boldsymbol{k}_{\boldsymbol{n}'})\mathrm{e}^{\mathrm{i}\boldsymbol{k}_{\boldsymbol{n}'}\cdot\boldsymbol{x}}\tilde{g}(\boldsymbol{x},\boldsymbol{k}-\boldsymbol{k}')\,\mathrm{d}v_{\boldsymbol{k}'} \\
&= \frac{|U|}{(2\pi)^3}\int_{U'} \tilde{f}(\boldsymbol{x},\boldsymbol{k}')\tilde{g}(\boldsymbol{x},\boldsymbol{k}-\boldsymbol{k}')\,\mathrm{d}v_{\boldsymbol{k}'} \qquad \text{(A.13)}
\end{aligned}
$$

Since $|U|/(2\pi)^3 = 1/|U'|$, this shows that the Floquet-Bloch transformation of a product is

$$[\widetilde{fg}](\boldsymbol{x},\boldsymbol{k}) = \frac{1}{|U'|}\int_{U'} \tilde{f}(\boldsymbol{x},\boldsymbol{k}')\tilde{g}(\boldsymbol{x},\boldsymbol{k}-\boldsymbol{k}')\,\mathrm{d}v_{\boldsymbol{k}'} = \frac{1}{|U'|}[\tilde{f} \overset{U'}{*} \tilde{g}](\boldsymbol{x},\boldsymbol{k}) \tag{A.14}$$

where we use the notation $\overset{U'}{*}$ to denote convolution over the reciprocal unit cell U'.

Appendix B Estimate of an integral operator

In this appendix we give an estimate of the integral operator

$$Ae_1 = \frac{1}{|U'|}\int_{U'} e_1(\boldsymbol{k}')\tilde{\zeta}_0(\boldsymbol{k}-\boldsymbol{k}')g(\boldsymbol{k},\boldsymbol{k}')\,\mathrm{d}v_{\boldsymbol{k}'} \tag{B.1}$$

The absolute value is

$$\begin{aligned}
|Ae_1| &= \left|\frac{1}{|U'|}\int_{U'} e_1(\boldsymbol{k}')\tilde{\zeta}_0(\boldsymbol{k}-\boldsymbol{k}')(s(\mathsf{M}_\mathrm{c}^\#-\mathsf{M}_0)\cdot \mathrm{e}^{\mathrm{i}\boldsymbol{k}\cdot\boldsymbol{x}}\mathsf{u}_1, \mathrm{e}^{\mathrm{i}\boldsymbol{k}'\cdot\boldsymbol{x}}\mathsf{v}_1)\,\mathrm{d}v_{\boldsymbol{k}'}\right| \\
&= \left|\left(s(\mathsf{M}_\mathrm{c}^\#-\mathsf{M}_0)\cdot\frac{1}{|U'|}\int_{U'} e_1(\boldsymbol{k}')\tilde{\zeta}_0(\boldsymbol{k}-\boldsymbol{k}')\mathrm{e}^{\mathrm{i}\boldsymbol{k}'\cdot\boldsymbol{x}}\mathsf{u}_1\,\mathrm{d}v_{\boldsymbol{k}'}, \mathrm{e}^{\mathrm{i}\boldsymbol{k}\cdot\boldsymbol{x}}\mathsf{v}_1\right)\right| \\
&\le \left\|s(\mathsf{M}_\mathrm{c}^\#-\mathsf{M}_0)\cdot\frac{1}{|U'|}\int_{U'} e_1(\boldsymbol{k}')\tilde{\zeta}_0(\boldsymbol{k}-\boldsymbol{k}')\mathrm{e}^{\mathrm{i}\boldsymbol{k}'\cdot\boldsymbol{x}}\mathsf{u}_1\,\mathrm{d}v_{\boldsymbol{k}'}\right\|_{L^2(U)} \left\|\mathrm{e}^{\mathrm{i}\boldsymbol{k}\cdot\boldsymbol{x}}\mathsf{v}_1\right\|_{L^2(U)} \\
&\le \left\|s(\mathsf{M}_\mathrm{c}^\#-\mathsf{M}_0)\right\|_{L^\infty(U)} \left\|\frac{1}{|U'|}\int_{U'} e_1(\boldsymbol{k}')\tilde{\zeta}_0(\boldsymbol{k}-\boldsymbol{k}')\mathrm{e}^{\mathrm{i}\boldsymbol{k}'\cdot\boldsymbol{x}}\mathsf{u}_1\,\mathrm{d}v_{\boldsymbol{k}'}\right\|_{L^2(U)}
\end{aligned} \tag{B.2}$$

where we used that v_1 has norm one over U. The relevant norm can then be estimated as

$$\begin{aligned}
&\frac{1}{|U'|}\left\|Ae_1\right\|_{L^2(U')}^2 = \frac{1}{|U'|}\int_{U'} |Ae_1|^2\,\mathrm{d}v_{\boldsymbol{k}} \\
&\le \left\|s(\mathsf{M}_\mathrm{c}^\#-\mathsf{M}_0)\right\|_{L^\infty(U)}^2 \frac{1}{|U'|}\int_{U'}\left\|\frac{1}{|U'|}\int_{U'} e_1(\boldsymbol{k}')\tilde{\zeta}_0(\boldsymbol{k}-\boldsymbol{k}')\mathrm{e}^{\mathrm{i}\boldsymbol{k}'\cdot\boldsymbol{x}}\mathsf{u}_1\,\mathrm{d}v_{\boldsymbol{k}'}\right\|_{L^2(U)}^2 \mathrm{d}v_{\boldsymbol{k}} \\
&= \left\|s(\mathsf{M}_\mathrm{c}^\#-\mathsf{M}_0)\right\|_{L^\infty(U)}^2 \frac{1}{|U'|}\int_{U'}\int_U\left|\frac{1}{|U'|}\int_{U'} e_1(\boldsymbol{k}')\tilde{\zeta}_0(\boldsymbol{k}-\boldsymbol{k}')\mathrm{e}^{\mathrm{i}\boldsymbol{k}'\cdot\boldsymbol{x}}\mathsf{u}_1\,\mathrm{d}v_{\boldsymbol{k}'}\right|^2 \mathrm{d}v_{\boldsymbol{x}}\,\mathrm{d}v_{\boldsymbol{k}} \\
&= \left\|s(\mathsf{M}_\mathrm{c}^\#-\mathsf{M}_0)\right\|_{L^\infty(U)}^2 \int_U \frac{1}{|U'|}\int_{U'}\left|\frac{1}{|U'|}\tilde{\zeta}_0 \overset{U'}{*} (e_1\mathrm{e}^{\mathrm{i}\boldsymbol{k}\cdot\boldsymbol{x}}\mathsf{u}_1)\right|^2 \mathrm{d}v_{\boldsymbol{k}}\,\mathrm{d}v_{\boldsymbol{x}} \\
&= \left\|s(\mathsf{M}_\mathrm{c}^\#-\mathsf{M}_0)\right\|_{L^\infty(U)}^2 \int_U \frac{1}{|U'|^3}\left\|\tilde{\zeta}_0 \overset{U'}{*} (e_1\mathrm{e}^{\mathrm{i}\boldsymbol{k}\cdot\boldsymbol{x}}\mathsf{u}_1)\right\|_{L^2(U')}^2 \mathrm{d}v_{\boldsymbol{x}}
\end{aligned} \tag{B.3}$$

For convolutions, we have the general estimate [12, p. 117]

$$\|f*g\|_{L^p} \le \|f\|_{L^1}\|g\|_{L^p} \tag{B.4}$$

which means

$$\frac{1}{|U'|}\left\|Ae_1\right\|^2_{L^2(U')} \leq \left\|s(\mathsf{M}_\mathrm{c}^\# - \mathsf{M}_0)\right\|^2_{L^\infty(U)} \int_U \frac{1}{|U'|^2}\left\|\tilde{\zeta}_0\right\|^2_{L^1(U')} \frac{1}{|U'|}\left\|e_1 \mathrm{e}^{\mathrm{i}\boldsymbol{k}\cdot\boldsymbol{x}}\mathsf{u}_1\right\|^2_{L^2(U')} \mathrm{d}v_{\boldsymbol{x}}$$
$$\leq \left\|s(\mathsf{M}_\mathrm{c}^\# - \mathsf{M}_0)\right\|^2_{L^\infty(U)} \left(\frac{1}{|U'|}\left\|\tilde{\zeta}_0\right\|_{L^1(U')}\right)^2 \frac{1}{|U'|}\left\|e_1\right\|^2_{L^2(U')}\left\|\mathsf{u}_1\right\|^2_{L^2(U)} \quad \text{(B.5)}$$

Thus, since $\|\mathsf{u}_1\|_{L^2(U)} = 1$ the norm of the integral operator can be estimated as

$$\|A\| \leq \left\|s(\mathsf{M}_\mathrm{c}^\# - \mathsf{M}_0)\right\|_{L^\infty(U)} \frac{1}{|U'|}\left\|\tilde{\zeta}_0\right\|_{L^1(U')} \quad \text{(B.6)}$$

The norm $\frac{1}{|U'|}\|\tilde{\zeta}_0\|_{L^1(U')}$ is O(1), which shows that the integral operator can be controlled at least in the weak contrast limit, where $\left\|s(\mathsf{M}_\mathrm{c}^\# - \mathsf{M}_0)\right\| \to 0$. Further analysis of this integral operator has not been performed yet.

References

[1] G. B. Arfken and H. J. Weber. *Mathematical Methods for Physicists.* Academic Press, New York, 1995.

[2] D. Bekers. *Finite Antenna Arrays: An Eigencurrent Approach.* PhD thesis, Technische Universiteit Eindhoven, 2004.

[3] E. Bleszynski, M. Bleszynski, and T. Jaroszewicz. AIM: adaptive integral method for solving large scale electromagnetic scattering and radiation problems. *Radio Sci.*, **31**, 1225–1251, 1996.

[4] F. Bloch. Über die Quantenmechanik der Electronen in Kristallgittern. *Z. Phys.*, **52**, 555–600, 1928.

[5] F. Capolino, M. Albani, S. Maci, and L. B. Felsen. Frequency-domain Green's function for a planar periodic semi-infinite phased array — part I: Truncated Floquet wave formulation. *IEEE Trans. Antennas Propagat.*, **48**(1), 67–74, January 2000.

[6] F. Capolino, M. Albani, S. Maci, and L. B. Felsen. Frequency-domain Green's function for a planar periodic semi-infinite phased array — part II: Diffracted wave phenomenology. *IEEE Trans. Antennas Propagat.*, **48**(1), 75–85, January 2000.

[7] R. Coifman, V. Rokhlin, and S. Wandzura. The fast multipole method for the wave equation: A pedestrian prescription. *IEEE Antennas and Propagation Magazine*, **35**(3), 7–12, 1993.

[8] L. C. Evans. *Partial Differential Equations.* American Mathematical Society, Providence, Rhode Island, 1998.

[9] G. Floquet. Sur les équations différentielles linéaries à coefficients périodique. *Ann. École Norm. Sup.*, **12**, 47–88, 1883.

[10] M. Gustafsson. *Wave Splitting in Direct and Inverse Scattering Problems.* PhD thesis, Lund Institute of Technology, Department of Electromagnetic Theory, P.O. Box 118, S-221 00 Lund, Sweden, 2000. `http://www.es.lth.se/home/mats`.

[11] M. Gustafsson. RCS reduction of integrated antenna arrays with resistive sheets. *J. Electro. Waves Applic.*, **20**(1), 27–40, 2006.

[12] L. Hörmander. *The Analysis of Linear Partial Differential Operators I.* Grundlehren der mathematischen Wissenschaften 256. Springer-Verlag, Berlin Heidelberg, 1983.

[13] A. Ishimaru, R. J. Coe, G. E. Miller, and W. P. Geren. Finite periodic structure approach to large scanning array problems. *IEEE Trans. Antennas Propagat.*, **33**(11), 1213–1220, November 1985.

[14] R. Kindt, K. Sertel, E. Topsakal, and J. L. Volakis. An extension of the array decomposition method for large finite-array analysis. *Microwave Opt. Techn. Lett.*, **38**(4), 323–328, August 2003.

[15] R. W. Kindt, K. Sertel, E. Topsakal, and J. L. Volakis. Array decomposition method for the accurate analysis of finite arrays. *IEEE Trans. Antennas Propagat.*, **51**(6), 1364–1372, June 2003.

[16] C. Kittel. *Introduction to Solid State Physics.* John Wiley & Sons, New York, 6 edition, 1986.

[17] B. Munk. *Finite Antenna Arrays and FSS.* John Wiley & Sons, New York, 2003.

[18] A. Neto, S. Maci, G. Vecchi, and M. Sabbadini. A truncated Floquet wave diffraction method for the full wave analysis of large phased arrays — part I: Basic principles and 2-D cases. *IEEE Trans. Antennas Propagat.*, **48**(3), 594–600, March 2000.

[19] A. Neto, S. Maci, G. Vecchi, and M. Sabbadini. A truncated Floquet wave diffraction method for the full wave analysis of large phased arrays — part II: Generalization to 3-D cases. *IEEE Trans. Antennas Propagat.*, **48**(3), 601–611, March 2000.

[20] D. Sjöberg. Homogenization of dispersive material parameters for Maxwell's equations using a singular value decomposition. *Multiscale Modeling and Simulation*, **4**(3), 760–789, 2005.

[21] D. Sjöberg, C. Engström, G. Kristensson, D. J. N. Wall, and N. Wellander. A Floquet-Bloch decomposition of Maxwell's equations, applied to homogenization. *Multiscale Modeling and Simulation*, **4**(1), 149–171, 2005.

[22] A. K. Skrivervik and J. R. Mosig. Finite phased array of microstrip patch antennas: The infinite array approach. *IEEE Trans. Antennas Propagat.*, **40**(5), 579–582, May 1992.

[23] A. K. Skrivervik and J. R. Mosig. Analysis of finite phase arrays of microstrip patches. *IEEE Trans. Antennas Propagat.*, **41**(8), 1105–1114, August 1993.

[24] A. K. Skrivervik and J. R. Mosig. Analysis of printed array antennas. *IEEE Trans. Antennas Propagat.*, **45**(9), 1411–1418, September 1997.

[25] J. M. Usoff and B. A. Munk. Edge effects of truncated periodic surfaces of thin wire elements. *IEEE Trans. Antennas Propagat.*, **42**(7), 946–953, 1994.